Desalination and Water Treatment
www.deswater.com

doi: 10.5004/dwt.2022.27959

245 (2022) 116–128
January

Removal of some hazardous ions using titanium oxide and *Cunninghamella elegans* immobilized in alginate–carboxymethyl cellulose beads

Mohamed Mahmoud E. Breky*, Alaa S. Abdel-Razek, Magda S. Sayed

Hot Laboratories and Waste Management Center, Egyptian Atomic Energy Authority (EAEA), 13759 Cairo, Egypt, emails: chemist_elbreky@yahoo.com (M.M.E. Breky), alasayabdelr@yahoo.com (A.S. Abdel-Razek), magdass7@hotmail.com (M.S. Sayed)

Received 20 May 2021; Accepted 31 October 2021

ABSTRACT

A series of batch tests using various adsorbents were conducted to remove hexavalent chromium (Cr^{6+}) and cobalt (Co^{2+}) ions from an aqueous solution. Hydrous TiO_2 and *Cunninghamella elegans* (*C. elegans*) were immobilized in sodium alginate–carboxymethyl cellulose (SA–CMC) gel beads to form adsorbents. Several gel (SA–CMC) ratios were examined to determine the optimum ratio. Scanning electron microscope, energy-dispersive spectroscopy, X-ray powder diffraction, and Fourier transform infrared (FTIR) spectrometry were used to characterize the resulted composite beads. The factors affecting the biosorption process, that is, pH, contact time, and initial feed concentration, on the Cr^{6+} and Co^{2+} ion sorption were also investigated. The results showed that the optimal Cr^{6+} removal efficiencies at pH = 2, adsorbent dosage = 5 g L^{-1}, initial feed concentration = 50 ppm, temperature = 30°C, and contact time = 180 min were 64% and 60% for *C. elegans*/SA–CMC gel beads (CESC) and TiO_2 gel beads (TSC), respectively. At the same conditions, except the pH (here, pH = 7), the optimal Co^{2+} removal efficiencies were 65% and 75% for CESC and TSC, respectively. The adsorption data of Cr^{6+} and Co^{2+} ions were studied using kinetic modeling and sorption isotherm models, which clearly confirmed that the pseudo-second-order kinetics and Langmuir isotherm are the best fit for the adsorption process. The maximum removal capacities of CESC were 200.64 and 187.78 mg/g and those of TSC were 220.34 and 142.21 mg/g for Cr^{6+} and Co^{2+}, respectively. HNO_3 (0.1 N) was found to be an effective reagent for the regeneration of the CESC and TSC sorbents, and the biosorbent could be reused for chromium and cobalt removal for up to three biosorption–desorption cycles. The outcomes of this research suggest that the proposed adsorbents are good candidates for the removal of Cr^{6+} and Co^{2+} ions from wastewater.

Keywords: Alginate; Carboxymethyl cellulose; Immobilization; Adsorption; Cr^{6+}; Co^{2+}

1. Introduction

Chromium has three oxidation states in nature: Cr^{2+}, C^{3+}, and Cr^{6+}. However, only C^{3+} and Cr^{6+} are stable [1,2]. Cr^{3+} is an essential nutrient for humans, of which the shortage may cause heart diseases, disruptions of glucose metabolisms, and diabetes. Cr^{3+} is relatively immobile, has low toxicity, and can be easily precipitated in nature [3]. Cr^{6+} is the most dangerous and toxic metal. It can be found in nature in the form of dichromate and strong oxides [4]. CrO_4^{2-} is a potent carcinogen and is extremely toxic to humans and animals [5]. It can cause several diseases such as lung cancer as well as kidney, liver, and gastric damage.

Various techniques have been developed for Cr^{6+} removal [6], including chemical precipitation [7], ion exchange resin [8], coagulation [9], reverse osmosis [10], membrane filtration [11], and adsorption [12]. Among these, adsorption using solid adsorbents is one of the most efficient methods

* Corresponding author.

for the treatment and removal of radioactive nuclides [13], toxic environmental contaminants [14], and organic pollutants [15]. Thus, adsorption is considered an excellent, simple, efficient, and relatively low-cost technique for mitigating even very low levels of herbicide pollution [16].

Biosorption is a green approach that uses naturally occurring biomass as sorbents for toxic metal ion sequestration [17,18]. Biosorption is a promising method that meets all the requirements of Cr^{6+} ion elimination from aqueous streams [19,20].

The International Atomic Energy Agency developed a set of laws and basic rules for managing radioactive wastes to protect the environment and human health [21]. Radioactive cobalt is a toxic radioactive element. It is one of the major contributors to the build-up of the radiation field that occurs in pressurized heavy water reactors [22]. ^{60}Co represents a serious concern because of its long half-life ($t_{1/2}$ = 5.27 y) and high gamma-emission energy (total is 2.5 MeV). Unlike heavy metals, radioactive elements can produce rays, which can enter the human body, causing internal contamination and posing various threats, including death. To prevent radioactive contamination, it is necessary to develop effective methods to remove radionuclides from radioactive wastewaters [13,23]. Conventional methods used for wastewater treatment include precipitation, solvent extraction, ion exchange, and membrane filtration [21,24].

Sodium alginate (SA) and carboxymethyl cellulose (CMC) are widely used as metal adsorbents because of their ability to form a gel through an ion exchange reaction with multivalent metal ions [25]. SA is a linear polymer containing blocks of 1,4-linked β-D-mannuronate (M block) and α-L-guluronate (G block) residues. The G blocks are easily crosslinked with metal ions, which induces gelation [26,27]. CMC is an ionic polysaccharide that contains carboxyl groups and can be used to prepare heavy metal adsorption materials [28]. SA/CMC gel has been used to immobilize TiO_2 because it is a nontoxic, inexpensive, and easily prepared immobilization carrier for enzymes and biomass materials.

Li et al. successfully synthesized a novel adsorbent by immobilizing TiO_2 on molecularly imprinted chitosan matrix for organic compound degradation and heavy metal adsorption [29]. No loss in the adsorbent material was observed after recycling and reusing the immobilized adsorbents compared with the pristine material. Another study reported that calcium alginate-immobilized TiO_2 beads showed excellent heavy metal (Pb^{2+} and Cd^{2+} ions) removal efficiency even after 10 adsorption–desorption cycles [30].

TiO_2 is typically used in a suspension form for metal ion adsorption in aqueous solutions [31–34]. Although this method is effective, large-scale water treatment using TiO_2 is impractical because suspended materials are difficult to separate from liquid streams, which causes continuous material losses during the recycling process [30]. Thus, as described here, immobilization of TiO_2 in SA–CMC resolves this problem.

Cunninghamella elegans (*C. elegans*) is a non-lignin-olytic fungus well known for its ability to transform a broad range of xenobiotics [35], and the inactivated biomass of the fungus is an effective biosorbent [36]. Composites of alginate with polyethyleneimine, gelatin, and CMC are also effective for Cr^{6+} removal.

In this study, TiO_2/SA–CMC (TSC) and *C. elegans*/SA–CMC (CESC) beads were developed and tested for the removal of Cr^{6+} and Co^{2+} ions from synthetic wastewater samples. The effects of the initial Cr^{6+} and Co^{2+} concentrations and initial solution pH on the Cr^{6+} and Co^{2+} removal were investigated. Equilibrium isotherms and kinetic modeling were employed to investigate the adsorption mechanism between Cr^{6+} and Co^{2+} ions with the TSC and CESC biosorbents. The reusability of the produced gel beads for Cr^{6+} and Co^{2+} recovery has been demonstrated using a simple technique.

2. Materials and methods

2.1. Chemical reagents

SA, CMC, and $TiCl_4$ were purchased from Fluka and used without further purification. Calcium chloride and cobalt solutions were prepared by the dissolution of $CaCl_2{\cdot}2H_2O$ and $CoCl_2{\cdot}6H_2O$, respectively, in distilled water. A stock solution of Cr^{6+} (1,000 mg/L) was prepared by dissolving the desired amount of $K_2Cr_2O_7$ in distilled water. Solutions with different Cr^{6+} concentrations were prepared via serial dilution of the stock solution using distilled water. The pH of the solutions was adjusted using analytical grade HCL (0.1 N) and NaOH (0.1 N).

2.2. Fungal isolates

C. elegans was isolated from the soil of the repository site of the Waste Management Facility, Hot Laboratory Center, operated by the Atomic Energy Authority of Egypt using the dilution plate method [37].

2.3. Preparation of hydrous TiO_2

Hydrolysis of $TiCl_4$ (0.3 mol/L) was conducted using NaOH (1 N) under continuous magnetic stirring. The pH of the solution was adjusted to 7.5 using NaOH (1 N), and the mixture was left to set for 16 h to generate a precipitate. It was then centrifuged, and the precipitate was washed three times with distilled water to remove any impurities. The residual precipitate was collected and dried at room temperature for 48 h. The dried precipitate was pulverized using agate mortar to obtain a fine powder.

2.4. Biomass production

The inocula of the fungal spore were transferred to 1-L conical flasks containing Sabouraud's broth occupying one-third of their volume. They were then incubated at 27°C for 3 d in an orbital shaking incubator. The cultivated fungal biomass was harvested by centrifugation and then washed several times with distilled water. The obtained fungal biomass was stored in a refrigerator to be used as living biomass [37].

2.5. Preparation of SA–CMC gel mixture

The SA gel (4%) was prepared by dissolving the sodium salt of alginic acid (4 g) in distilled water (100 mL)

with gentle stirring for 5 h. CMC gel (4%) was prepared by dissolving the sodium salt of CMC (4 g) in distilled water (100 mL) with gentle stirring for 5 h. Different gel ratios (20%, 40%, 60%, and 80%) of SA and CMC were prepared under constant stirring to generate a homogeneous gel mixture.

2.6. Preparation of TSC gel beads

Different masses (0.02, 0.04, 0.05, 0.06, 0.08, and 0.1 g) of TiO_2 were added to the prepared SA–CMC gel mixture (10 mL) under continues magnetic stirring. Next, the mixture was dropped into a $CaCl_2$ solution (2%, 250 mL) using a peristaltic pump, and the resulted beads were allowed to solidify for 24 h. The coagulated beads were then washed several times with distilled water to remove the excess calcium. The beads were divided into two parts, of which one was gently stirred in an $FeCl_3$ solution (1%, 100 mL) to further solidify for 24 h. The resulted gel beads were washed several times with distilled water, and the beads were then dried at room temperature for 48 h (Fig. 1).

2.7. Preparation of CESC beads

Different masses of the fungal mycelia (i.e., 0.125, 0.05, 0.1, 0.2, 0.3, 0.4, and 0.5 g) were ground and mixed thoroughly in the prepared SA–CMC gel mixture (10 mL) under continuous magnetic stirring. Then, the mixture was dropped into a $CaCl_2$ solution (2%, 250 mL) using a peristaltic pump, and the resulted beads were allowed to solidify for 24 h. The coagulated beads were then washed several times with distilled water to remove the excess calcium. The beads were divided into two parts, of which one part was gently stirred in an $FeCl_3$ solution (1%, 100 mL) to further solidify for 24 h. The resulted gel beads were washed several times with distilled water, and then, the beads were dried at room temperature for 48 h.

2.8. Characterization

The dried samples were characterized using various spectroscopic methods. The surface morphology and elemental composition of the composite adsorbent were studied using scanning electron microscope (SEM, FEI Quanta FEG 250, USA) and energy-dispersive X-ray spectrometry (EDS, EDAX APOLLO X, USA). A Fourier transform infrared (FTIR) spectroscopy (Nicolet 6700, Thermo Electron Scientific Instruments Corporation, USA) was used in an attenuated total reflection mode to record FTIR spectra using KBr pellets. X-ray diffraction (XRD) was recorded at room temperature using a powder diffractometer (Bruker axs D8 Advance, Germany) with a Cu Kα radiation source (k = 1.5406 Å) and 2θ in the range of 10–80. The porous structures of CESC and TSC were characterized by the adsorption–desorption of the N_2 Brunauer–Emmett–Teller (BET) method (JEOL-JSM 6510 LA, Japan) at the temperature of liquid nitrogen (77°K).

2.9. Sorption study

The sorption performance of TSC and CESC beads for the removal of Cr^{6+} and Co^{2+} ions was studied in batch mode and then compared. The studies were performed in capped glass tubes (25 mL). The sorbate solutions (10 mL) at the desired concentrations were equilibrated with the sorbents (0.05 g, TSC beads or CESC beads) in a shaker at 50 rpm. The beads were separated after reaching equilibrium, and the residual metal concentration in the filtrate

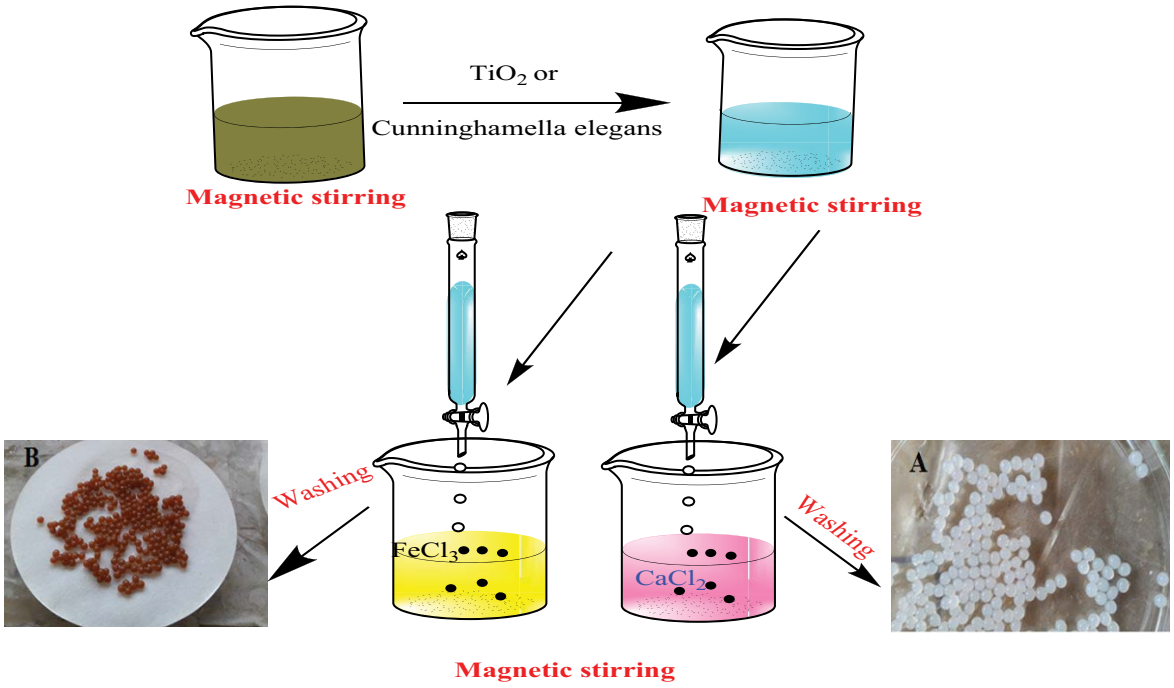

Fig. 1. Schematic diagram illustrating the synthesis of TSC and CESC gel beads.

was determined using atomic absorption spectrophotometer (Buck model 210 VGP).

The Cr^{6+} and Co^{2+} removal efficiency is defined as the ratio of Cr^{6+} and Co^{2+} ions adsorbed on the sorbent to that of the initial quantity of Cr^{6+} and Co^{2+} ions in the solution. The sorption capacity (mg/g) is defined as the uptake amount of Cr^{6+} and Co^{2+} ions per unit mass of the sorbent.

The removal efficiency of Cr^{6+} and Co^{2+} and the adsorption capacity at equilibrium (q_e, mg/g) were determined using Eqs. (1) and (2) [23]

$$\text{Adsorption}\left(\%\text{ removal efficiency}\right)=\frac{C_i-C_e}{C_i}\times 100 \quad (1)$$

$$\text{Removal capacity}\ \left(\text{mg/g}\right) q_e=\frac{C_i-C_e}{W}\times V \quad (2)$$

where C_i and C_e are the initial and equilibrium concentrations (mg/L) of the adsorbate, respectively, W (g) is the dry mass of the adsorbent, and V (L) is the volume of the solution. pH studies were conducted in a pH range of 2–10 and 2–8 for Cr^{6+} and Co^{2+}, respectively, at room temperature (303 K). The initial pH of the sorbate solution was adjusted using HCl (0.1 M) and NaOH (0.1 M) solutions. Contact-time studies were conducted at an initial sorbate concentration of 50 mg/L at room temperature.

2.10. Biosorbent reusability

The ability of the biosorbent to regenerate is a critical factor affecting the commercial success and industrial use of TSC and CESC beads [20]. Thus, the regeneration capability of spent TSC and CESC beads was investigated using different solvents such as double distilled water, NaOH solution (0.1 N), and HNO_3 solution (0.1 N). The beads were then washed in double distilled water until the pH of the washing water reached 6–6.5. The beads were reused three times in succession. The desorption ratio was calculated using the concentration of metal ions in the eluted solution.

3. Results and discussion

3.1. The effect of different content ratios of beads on the adsorption process

3.1.1. Ratio of SA and CMC

To investigate the optimum mass ratio between SA and CMC, adsorbents were synthesized at different mass ratios (SA:CMC = 80:20, 60:40, 50:50, 40:60, and 20:80). $CaCl_2$ and $FeCl_3$ were used in the solidification of the prepared adsorbents. The visual assessment showed that $FeCl_3$ increased the hardness and decreased the flexibility of the beads. Thus, the beads were easily destroyed during the sorption experiments. Therefore, only $CaCl_2$ was sufficient for the solidification process, and there was no need to use $FeCl_3$. Moreover, the strength of the beads decreased with the increase in the percentage of CMC in the gel mixture, and it was found that the SA:CMC ratio (50:50) was the ideal ratio for the gel mixture.

3.1.2. Ratio of TiO_2 and C. elegans

To investigate the optimum mass of TiO_2 and *C. elegans* immobilized in the SA–CMC beads, different mass ratios were studied to determine their adsorption capacity for Cr^{6+} and Co^{2+}. Finally, the ideal content ratio for TiO_2 and *C. elegans* was determined to be 0.05 and 0.125 g, respectively. Fig. 2 shows the adsorption capacity of Cr^{6+} and Co^{2+} over different mass ratios of TiO_2 and *C. elegans*. The adsorption capacity of Cr^{6+} and Co^{2+} increased with the increase in the content of TiO_2 from 0.02 to 0.04 g and decreased at 0.06, 0.8, and 0.1 g. However, the SA–CMC modified adsorbent exhibited lower adsorption capacity for Cr^{6+} and Co^{2+} with the increase in the mass ratio of *C. elegans* from 0.1 to 0.5 g. This can be attributed to the reduction in the active sites on the gel composite beads with the increase in the ratio of *C. elegans* to TiO_2 [23].

3.2. SEM results

Fig. 3 shows the SEM images of TSC and CESC beads. The TSC and CESC beads were spherical in shape with a porous surface structure, which enables the solution to easily penetrate. The CESC beads were pale yellow, whereas the TSC was white because of the encapsulation of TiO_2. Both surfaces of TSC and CESC beads were rough and porous. The SEM results were obtained to characterize the porous structure and rough surface of TSC and CESC beads.

3.3. FTIR results

FTIR was used to characterize the functional groups on the biosorbent surface within a range of 400–4,000 cm^{-1}. Characteristic peaks of various bonds were observed. These bonds were formed as a result of the biosorption on the material surfaces through the interaction of numerous functional groups of polysaccharides, such as amines, amides, and carboxylates, in the SA and CMC beads (Fig. 4). Fig. 4 shows a comparison between the FTIR spectra of CESC and TSC. All major peaks of CESC occurred at 3,440; 2,937; 1,668; 1,450 and 1,117 cm^{-1}, which have been assigned to the O–H stretching, –CH stretching, asymmetric vibration of –COO, symmetric vibration of –COO, and C–O–C stretching, respectively. The peak at 494 cm^{-1} was assigned to the stretching of the Ti–O–O bonds, which confirmed the presence of strong interactions between the polar sites of TiO_2 and the active functional sites of the biopolymer.

3.4. XRD results

The crystallinity of the TSC and CESC samples was investigated using an XRD pattern (Fig. 5). The XRD pattern of the TSC sample revealed three distinct peaks at 25.212°, 47.855°, and 37.716°, confirming the presence of an anatase phase (36.9%), and the second TiO_2 phase was a brookite phase (63.1%). The XRD pattern indicated that the CESC had an amorphous structure with a degree of crystallinity = 28.01%.

Higher crystallinity reduces porosity and surface area, resulting in a "cleaner" surface with fewer moieties and defects. As these defects are energetic locations for

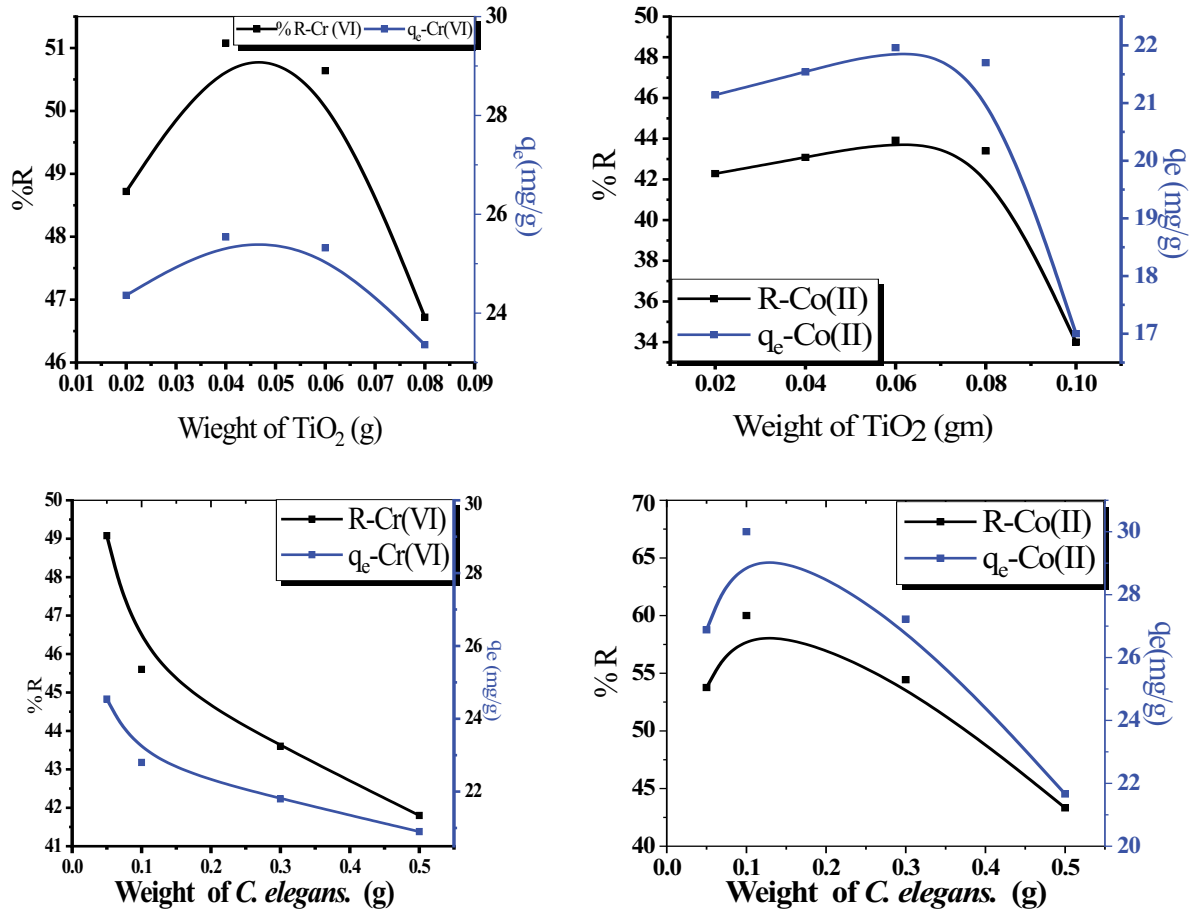

Fig. 2. The effect of immobilized TiO_2 and *C. elegans* content on the uptake of Cr^{6+} and Co^{2+} (contact time = 180 min, initial concentration = 50 mg/L).

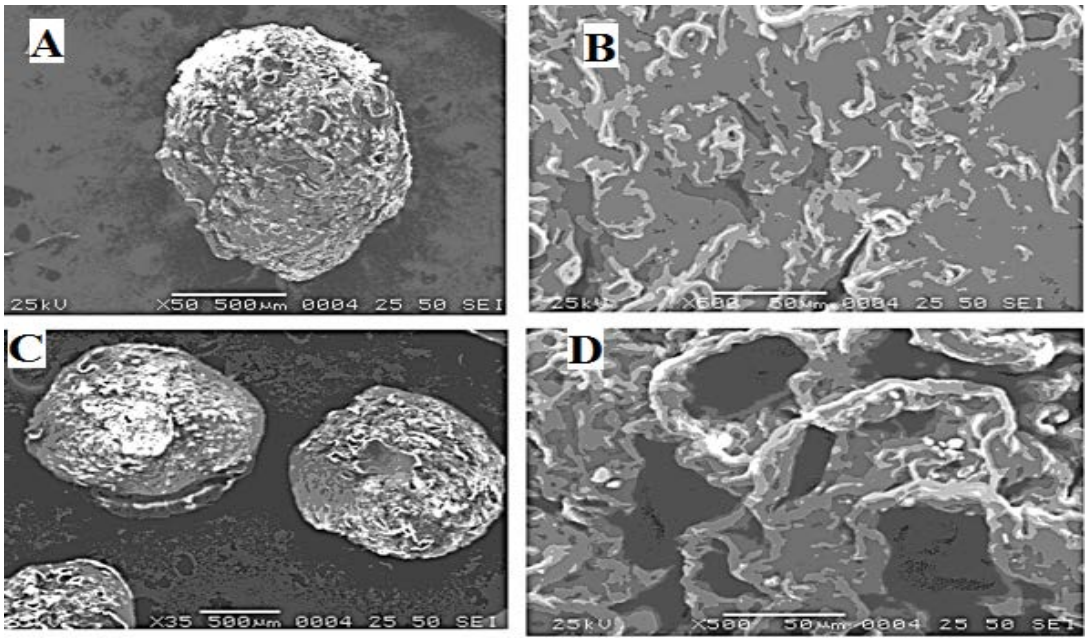

Fig. 3. The SEM images of TSC beads (A, B) and CESC gel beads (C, D).

adsorption, CESC (with low crystallinity) exhibited higher adsorption capacity.

3.5. EDS results

EDS was used to study the elemental composition of the biosorbent (Fig. 6). On the basis of EDS elemental analysis, the following elements were identified: C, O, Ca, Ti, Cr, and Co. Titanium was easily identified in the EDS spectra of the SA–CMC sample crosslinked with Ti after the Co^{2+} and Cr^{6+} ion removal. These results confirm the adsorption and binding of Co^{2+} and Cr^{6+} ions (Fig. 6).

3.6. Textural characteristics

Type IV class and H_2-type hysteresis were observed in the isotherm, which reflect the complex pore structure of the CESC and TSC biosorbents (Fig. 7) [18,38]. The specific surface areas of CESC and TSC were estimated on the basis of the multipoint BET method to be 39.5 and 0.414 m^2/g, respectively. Moreover, the mean pore radii of CESC and TSC were estimated to be 0.0106 and 0.696 nm, respectively, and the total pore volumes of CESC and TSC were 0.105 and 0.072 cm^3/g, respectively [38]. These suitable specific surface areas, pore volumes, and pore sizes were expected to generate superior biosorption of the target molecules, that is, Cr^{6+} and Co^{2+} ions.

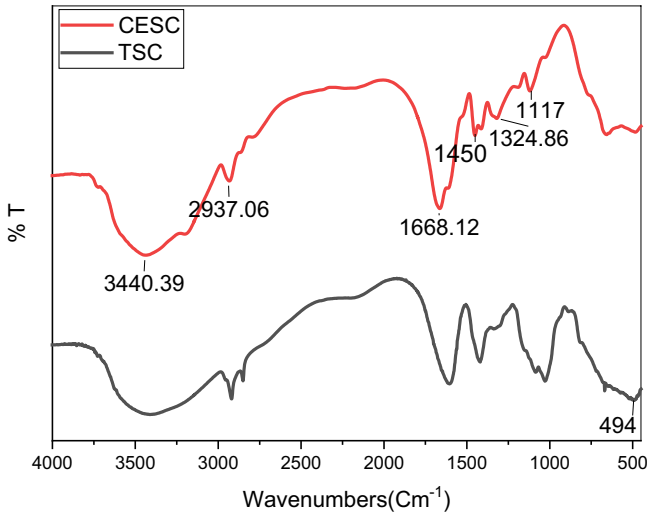

Fig. 4. The FTIR spectrum of the prepared TSC and CESC beads.

4. Effect of initial solution pH

pH is an important factor affecting the removal of Cr^{6+} and Co^{2+} ions from aqueous solutions. The dependence of metal sorption on pH is attributed to the metal chemistry in the solution and the ionization state of the functional groups of the sorbent, which affects the availability of binding sites [39]. The effect of pH on Cr^{6+} and Co^{2+} removal by TSC and CESC beads was examined at a pH range of 2–10 and 2–8, respectively.

The adsorption of Cr^{6+} ions decreased with the increase in the pH value. At pH = 3, the maximum adsorption percentages were 65% and 60% for the TSC and CESC beads, respectively. This behavior can be explained by taking into account the surface charge of the prepared beads and Cr^{6+} ions at different pH values. At low pH values, the surfaces of TSC and CESC beads are possibly covered by protons, forming positively charged particles. Fig. 8 indicates that Cr^{6+} is dominantly present as $HCrO_4^{-1}$, resulting in an increase in the electrostatic interaction between the negative Cr^{6+} species and the positive surface of the adsorbent [40]. The speciation diagram in Fig. 8 also shows the species formed in the aqueous media by the hexavalent chromium ($HCrO^{-4}$). At high pH values, there is a remarkable decrease in the Cr^{6+} removal, which may be attributed to the electrostatic repulsion between CrO_4^{-2} and the negatively charged surface of the deprotonated beads. This repulsion could be attributed to the reaction between the hydrous oxide and the highly concentrated hydroxide ions in the alkaline solution [41].

Fig. 9 shows the removal of cobalt. As expected, highly acidic conditions caused low adsorption of metal ions. The protonation of binding sites under highly acidic

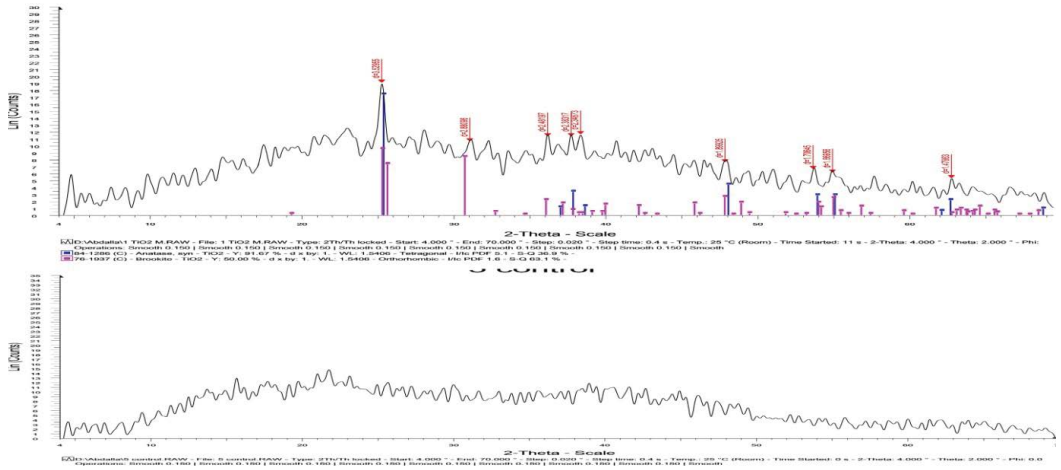

Fig. 5. X-ray diffraction patterns of TSC and CESC beads.

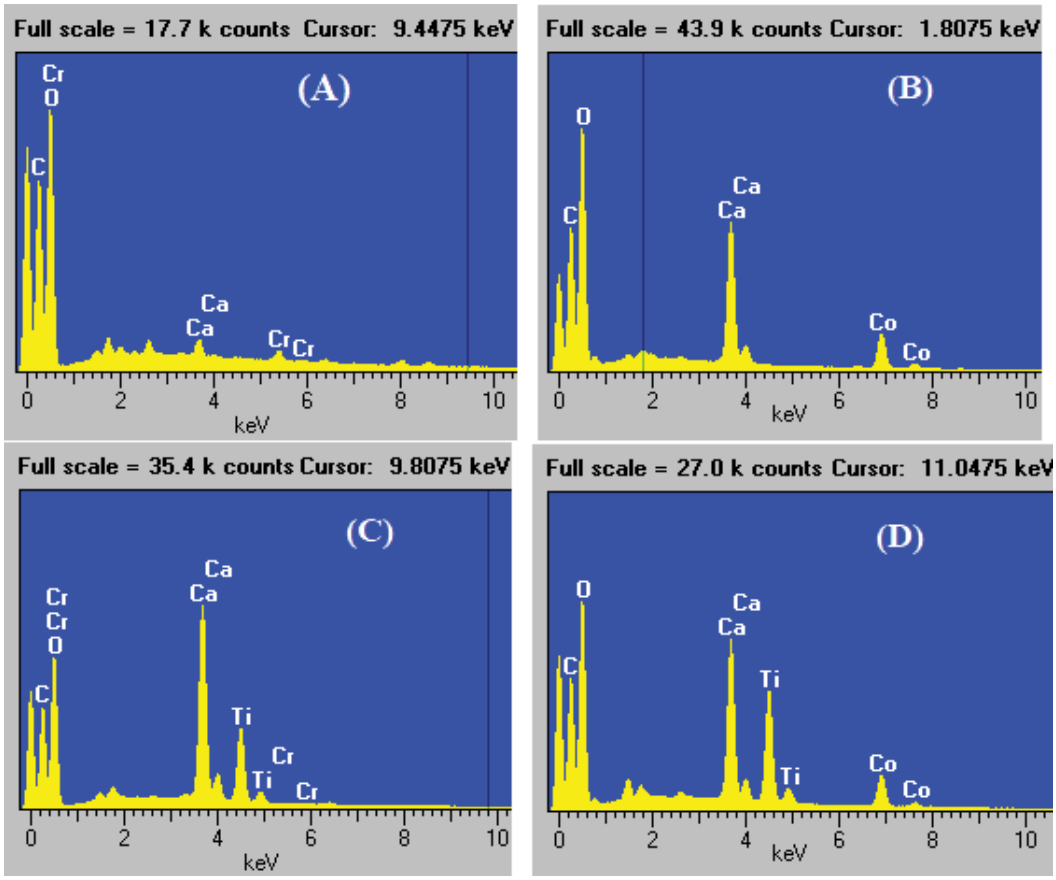

Fig. 6. EDS spectra of the CESC beads crosslinked with calcium chloride after (A) Cr^{6+} and (B) Co^{2+} adsorption as well as those of TSC after (C) Cr^{6+} and (D) Co^{2+} adsorption.

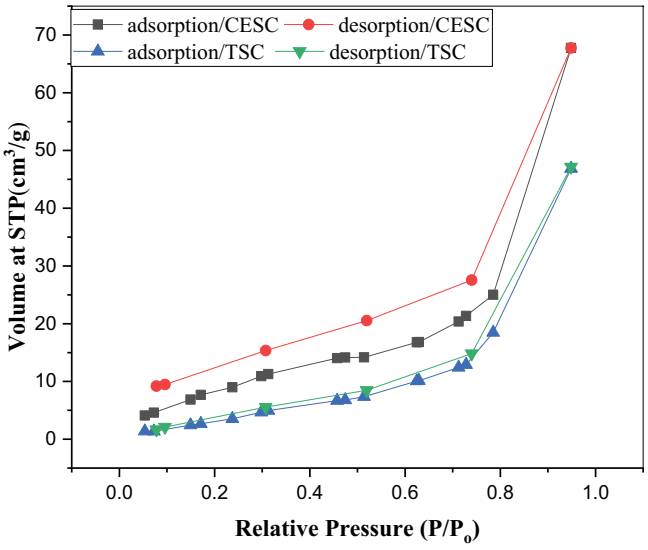

Fig. 7. N_2 adsorption–desorption patterns for CESC and TSC.

conditions resulted in a competition between H^+ and cationic metal ions for the binding sites, leading to low sorption. Increasing the pH from 2 to 4 improved the metal sorption, which might be attributed to the decrease in the number of H^+ ions competing with the metal cations for the sorption sites. A further increase in the pH from 4 to 8 resulted in a slow but constant increase in the sorption rate. The maximum metal ion uptake was observed at pH = 8.

4.1. Equilibrium and isotherm study

The equilibrium studies were conducted for the removal of Cr^{6+} and Co^{2+} by TSC and CESC at different initial concentrations of Cr^{6+} and Co^{2+} (100–1,000 mg/L) under optimized conditions. The equilibrium status in the metal ion removal process is determined on the basis of the distribution of the metal ions between the liquid and solid phases. The equilibrium data were analyzed via a nonlinear regression method using Langmuir and Freundlich models. Langmuir isotherm is a useful isotherm model for describing both physical and chemical sorption processes. A basic assumption of the Langmuir theory is that sorption takes place at specific homogeneous sites within the sorbent. The nonlinear form of this model is given in Eq. (3) [42]:

$$q_e = \frac{K_L q_{\max} C_e}{\left(1 + K_L C_e\right)} \tag{3}$$

where q_e is the metal ion concentration on the sorbent (mg/g) at equilibrium, C_e is the metal ion concentration in the

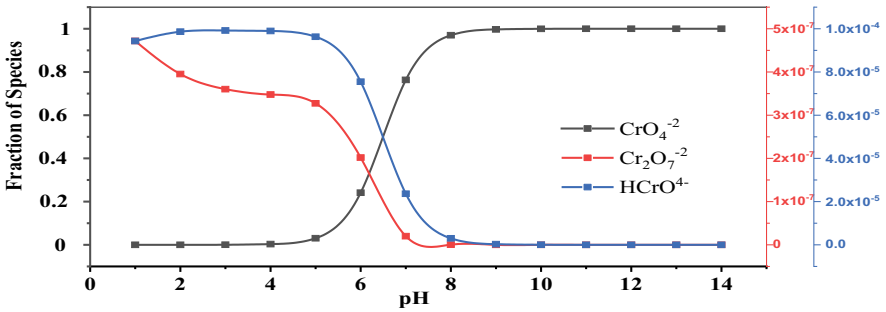

Fig. 8. Speciation diagram of Cr^{6+} at a concentration of 50 mg/L and room temperature.

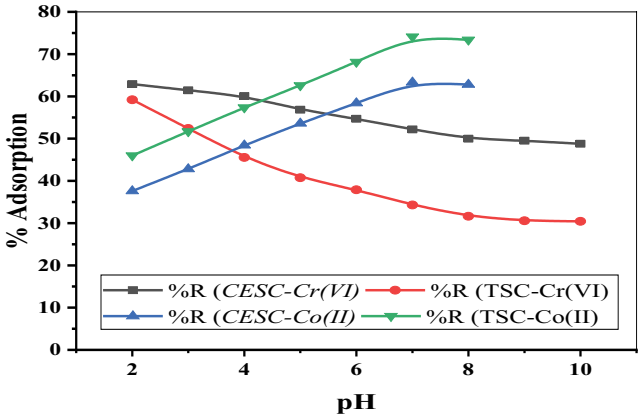

Fig. 9. Effect of pH on the removal of Cr^{6+} and Co^{2+} ions from aqueous solutions (adsorbent dosage = 5 g/L and C_i = 50 ppm).

solution (mg/L) at equilibrium, q_{max} is the monolayer sorption capacity of the sorbent (mg/g), and K_L is the Langmuir adsorption constant (mass transfer coefficient, L/mg), which depends on the free energy of sorption.

The Freundlich isotherm model assumes a heterogeneous adsorption surface and active sites with different energies. The Freundlich model is given in Eq. (4) [43]:

$$q_e = K_F C_e^{1/n} \quad (4)$$

where K_F ($mg^{(1-n)}$ L^n g^{-1}) is the Freundlich constant, which depends on the quantity of the sorbent, and $1/n$ is the affinity of the binding sites.

The results obtained for the isotherm studies are presented in Fig. 10 and Table 1. Fig. 10 shows the isotherm fitting curves which indicate that the Langmuir isotherm model is best suited for adsorptive remediation of Cr^{6+} and Co^{2+} by the TSC and CESC beads. The maximum adsorption capacity (q_{max}) was calculated from the Langmuir isotherm model (Table 1), which suggests a monolayer-type adsorption and an energetically uniform surface [44].

5. Effect of contact time

The contact time between the adsorbent and metal ions is another key parameter in the adsorption process. In practice, the contact time must be optimized because it affects the adsorption kinetics and directly reflects the economic efficiency of the process. The effect of the shaking time on Cr^{6+} and Co^{2+} distribution is tested to clarify its effect on the reaction kinetics. The sorption kinetics of Cr^{6+} and Co^{2+} was studied at different time intervals ranging from 15 min to 24 h at a constant V/M ratio. Fig. 11

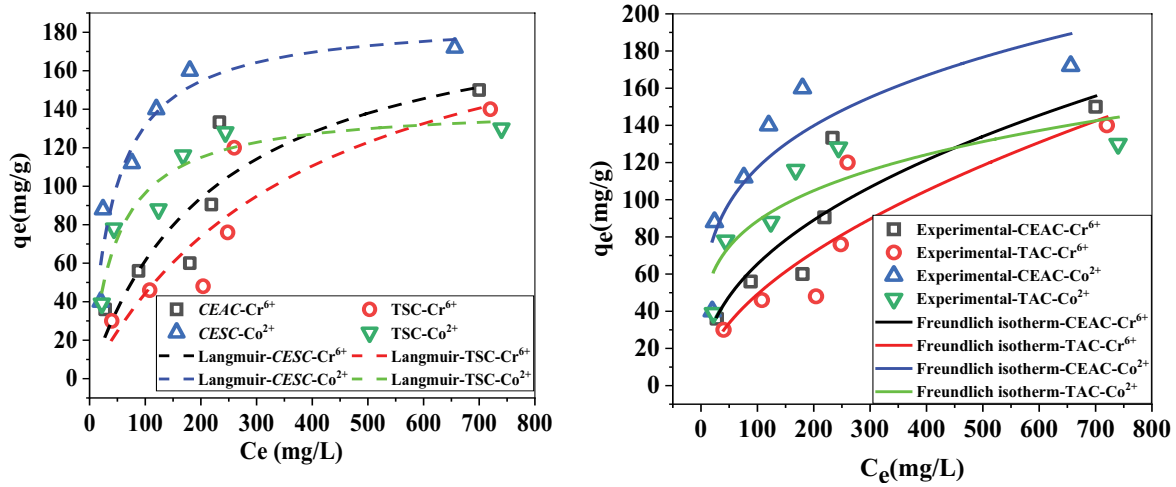

Fig. 10. Langmuir and Freundlich isotherm plots for the removal of Cr^{6+} and Co^{2+} by (A) TSC and CESC; experimental conditions: pH = 2 for Cr^{6+} and pH = 6 for Co^{2+}, t = 180 min, T = 25°C, M(TSC) = 5 g/L, M(CESC) = 5 g/L (The same symbols were used for the two figures).

Table 1
Parameters used for the Langmuir and Freundlich isotherm models employed for Cr^{6+} and Co^{2+} adsorption on CESC and TSC beads

Metal ion/ Sorbent	Langmuir model			Freundlich model		
	q_{max} (mg/g)	K_L (L/mg)	R^2	K_F (mg$^{(1-n)}$ L^n g^{-1})	n	R^2
CESC-Cr^{6+}	200.64	0.0044	0.79978	8.35987	2.23969	0.79535
TSC-Cr^{6+}	220.34	0.00252	0.79939	3.95713	1.82848	0.79099
CESC-Co^{2+}	187.78	0.02331	0.92042	36.17641	3.91896	0.78317
TSC-Co^{2+}	142.21	0.02107	0.92467	28.69196	4.0876	0.78802

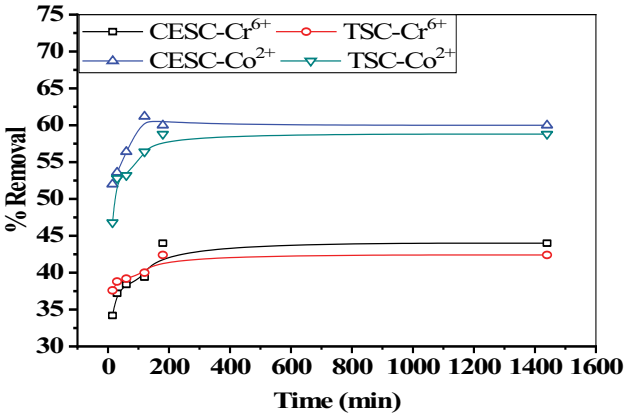

Fig. 11. Effect of contact time on the removal of Cr^{6+} and Co^{2+} using CESC and TSC adsorbent from aqueous solutions (adsorbent dosage = 5 g L^{-1}, C_i = 50 ppm, pH = 2 for Cr^{6+}, and pH = 6 for Co^{2+}).

indicates that the equilibrium time of Cr^{6+} and Co^{2+} sorption on the TSC and CESC beads was 3 h.

5.1. Kinetic study

For Cr^{6+} and Co^{2+} adsorption from aqueous solutions, the rate of adsorption is an important parameter for the design and assessment of adsorbent capacity. Adsorption kinetic experiments were carried out to understand the adsorption mechanism of Cr^{6+} and Co^{2+} ions using the CESC and TSC [45].

The kinetics of Cr^{6+} and Co^{2+} removal by TSC and CESC was studied using pseudo-first-order and pseudo-second-order models. The linear form of the pseudo-first-order model is given in Eq. (5) [46]. The linear forms of the pseudo-first-order and pseudo-second-order equations are expressed using Eqs. (5) and (6), respectively.

$$\ln\left(q_e - q_t\right) = \ln q_e - K_1 t \tag{5}$$

where q_e and q_t (both in mg/g) are the amounts of metal ions removed per unit mass of the sorbent at equilibrium and at time t (min), respectively, and K_1 (min^{-1}) is the rate constant of the pseudo-first-order kinetics. The value of K_1 was calculated from the slope of the linear plot of $\ln(q_e - q_t)$ vs. t (Fig. 12a). The experimental data were also analyzed using the pseudo-second-order model, of which the linear form is given using Eq. (6) [47]:

$$\frac{t}{q_t} = \frac{1}{K_2 q_e^{\,2}} + \frac{1}{q_e} t \tag{6}$$

where K_2 (g/mg min) is the rate constant of the pseudo-second-order model, q_e and q_t (mg/g) are the number of metal ions removed per unit mass of the sorbent at equilibrium and at time t (min), respectively. The constants in the equations were calculated from the linear plots of t/q_t vs. t (Fig. 12b). The constants and correlation coefficients of the kinetic models are listed in Table 2.

As seen in Table 2, the values of the correlation coefficients indicated a better fit of the pseudo-second-order model with the experimental data compared with the pseudo-first-order model, indicating that the chemisorption [48] is the rate-determining step for the sorption of Cr^{6+} and Co^{2+} on CESC and TSC conducted in this study.

5.2. Thermodynamics of the biosorption

The thermodynamic characteristics of the current system were established in order to obtain insights into the thermodynamics of the sorption process. The essential requirement of the spontaneity is the change in the Gibbs free energy, ΔG. If ΔG is negative at a given temperature, the reaction would be spontaneous. The Van't Hoff equation was used to determine the thermodynamic parameters as follows

$$\Delta G^\circ = -RT \ln K_L \tag{7}$$

$$\ln K_L = \frac{\Delta S^\circ}{R} - \frac{\Delta H^\circ}{RT} \tag{8}$$

where R is the universal gas constant, T is the system absolute temperature (K), and K_o is the standard thermodynamic equilibrium constant (L/g) defined by q_e/C_e. The values of ΔH° and ΔS° were calculated from the slope and intercept of a plot of $\ln K_L$ vs. $1/T$ (Fig. 13), respectively, and the findings are listed in Table 3.

ΔG° values for the synthesized CESC and TSC beads were negative, indicating a spontaneous adsorption process. The values of ΔH° were positive, indicating that the sorption of Cr^{6+} and Co^{2+} ions is endothermic. The possibility of Cr^{6+} and Co^{2+} ion diffusion into the particles could not be ruled out because the synthesized adsorbents are porous. As a result, the increase in the temperature affects the diffusion of Cr^{6+} and Co^{2+} ions within the pores of the adsorbents. The number of active sites formed in the adsorbent increased with the temperature, indicating an increase

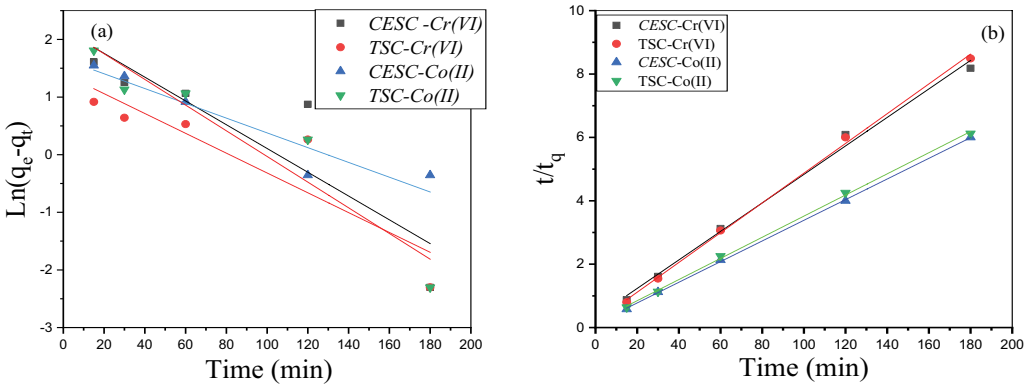

Fig. 12. Plots of (a) pseudo-first-order and (b) pseudo-second-order kinetic models for the sorption of Cr^{6+} and Co^{2+} ions on CESC and TSC gel beads at T = 30°C, m = 5 g/L, and C_i = 50 mg/L.

Table 2
Kinetic parameters of the pseudo-first-order and pseudo-second-order kinetic models for the sorption of Cr^{6+} and Co^{2+}

	Pseudo-first-order				Pseudo-second-order		
Sorbent	$q_{e,exp}$ (mg/g)	$q_{e,cal}$ (mg/g)	K_1 (min^{-1})	R^2	$q_{e,cal}$ (mg/g)	K_2 (g/mg min)	R^2
CESC-Cr^{6+}	22	8.77	0.0001	0.718	22.24	0.006030958	0.992
TSC-Cr^{6+}	21.2	4.07	9.55556E-05	0.737	21.30	0.012454715	0.997
CESC-Co^{2+}	30	5.26	7.12222E-05	0.872	30.68	0.008516623	0.99965
TSC-Co^{2+}	29.4	9.01	0.000123778	0.872	29.98	0.006175173	0.9988

Table 3
Thermodynamic parameters of Cr^{6+} and Co^{2+} ion biosorption on CESC and TSC surfaces

Adsorbent	Ions	Temperature (K)	$\Delta G°$ (kJ/mol)	$\Delta H°$ (kJ/mol)	$\Delta S°$ (J K^{-1} mol^{-1})
CESC	Cr(VI)	303	–3.469678996	10.86745388	47.22751072
		313	–3.856712232		
		323	–4.417938103		
TSC	Cr(VI)	303	–2.584269213	8.861479145	37.77640494
		313	–2.963620319		
		323	–3.33972853		
CESC	Co(II)	303	–4.69371181	15.69593467	67.00618416
		313	–5.091818872		
		323	–6.045668524		
TSC	Co(II)	303	–2.431175819	6.451496223	33.5058357
		313	–2.710156672		
		323	–3.103732071		

in the sorption capacity. Furthermore, positive $\Delta S°$ values indicate that the synthesized adsorbents have a high binding affinity for Cr^{6+} and Co^{2+} ions, and it also indicates a high randomization at the adsorbent–adsorbate interface during the sorption process [49].

6. Maximum retention capacity of the sorbents for Cr6+ and Co2+ ions

The effect of the metal ion concentration on the adsorption capacity of Cr^{6+} and Co^{2+} ions on TSC and CESC beads was studied at different concentrations while keeping the other parameters constant. Fig. 14 shows the retention capacities of Cr^{6+} and Co^{2+} ions on TSC and CESC beads as a function of their concentrations (from 100 to 1,000 ppm) at pH = 4. The equilibrium capacity of Cr^{6+} and Co^{2+} ions increased with the increase in the added amounts of metal ions. The removal efficiency decreased with the increase in the initial metal ion concentration when the amount of the adsorbent is kept unchanged. This can be attributed to the saturation of the adsorption sites on the adsorbent surface at high metal ion concentrations [50,51]. In addition,

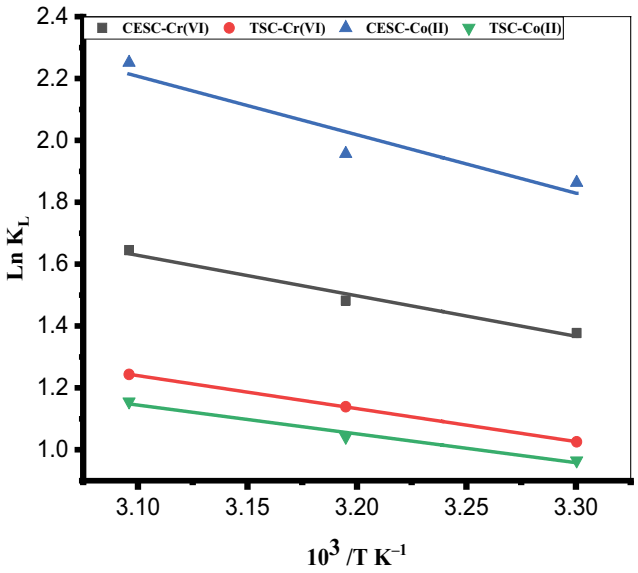

Fig. 13. Plot of ln *K* vs. 1/*T* for sorption of Cr^{6+} and Co^{2+} ions on CESC and TSC.

high initial metal concentrations cause a high driving force, which completely overcomes the mass transfer resistance of the metal ions at the interface between the aqueous and solid phases. This leads to higher probability of collision between the metal ions and adsorbent, which consequently increases the loading capacity of the adsorbent [52,53]. The adsorption capacities of Cr^{6+} ions on CESC and TSC at equilibrium were found to be 140 and 130 mg/g, respectively. The maximum adsorption capacities of Co^{2+} ions on CESC and TSC were found to be 160 and 120 mg/g, respectively. In the previous case, the adsorbent (CESC and TSC) dose did not change while the adsorbate concentration was increasing. In this situation, additional vacant sites on the CESC and TSC are occupied by the adsorbate molecules due to the higher concentrations. These values are considerably higher than those obtained in other reported studies using various kinds of sorbents (Table 4).

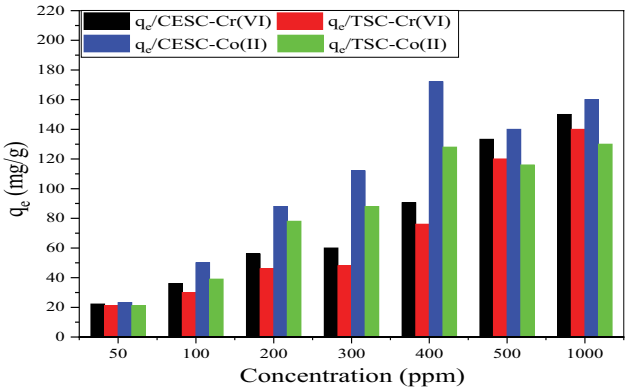

Fig. 14. Sorption isotherm of Cr^{6+} and Co^{2+} ions on TSC and CESC beads at pH = 2 for Cr^{6+} and pH = 6 for Co^{2+}, and V/M = 0.2 L/g.

7. Biosorbent reusability

The reusability of the biosorbent is one of the strategic parameters that impact the economic viability of the biosorption system and reduces the operation expenses of the separation process.

Fig. 15 illustrates the results of the reusability studies of CESC and TSC biosorbents. The desorption ratio after the first cycle was lower than that after the other cycles. The biosorbent was regenerated using HNO_3 (0.1 N) and then effectively reused for a maximum of three cycles. A significant reduction in the biosorption potential in cases of CESC and TSC (regenerated using HNO_3, 0.1 N) was observed when they were used for more than three cycles caused by the decrease in the surface functional groups due to chemical regeneration and continual saturation of the binding sites [20,62]. Thus, the reusability analysis showed that CESC and TSC could be repeatedly used up to three successive biosorption–desorption cycles.

8. Conclusions

CESC and TSC absorbents were used as novel biosorbents for the removal of Cr^{6+} and Co^{2+} ions from aqueous

Table 4
Comparison between the adsorption capacities of the prepared sorbents and those reported in the literature

Adsorbent		q_e (mg/g)		Reference
	pH, dosage, contact time	Cr(VI)	Co(II)	
TSC beads	pH 2 for Cr^{6+} and 6 for Co^{2+}, 0.05 g t.180 min	130	120	Present study
CESC beads		140	160	
Tetraethylenepentamine-SA beads (TEPA-SA)	2, 0.2 g, 180 min	76.92		[54]
PVA/chitosan magnetic composite	6, 0.03 g, 18 h		14.39	[55]
Thiourea-immobilized polymer beads	1, 0.03 g, 24 h	137		[56]
Modified chitosan beads	90 min		7.97	[57]
Chitosan-coated sour cherry kernel shell beads		24.49		[58]
Poly(amidoxime) modified reduced graphene oxide			177.6	[59]
Chitosan microspheres/sodium alginate hybrid beads	pH 3, 220 min, 0.06 g	16		[60]
Graphite nano carbon/alginate	pH 5, 8 h, 0.2 g		11.63	[61]

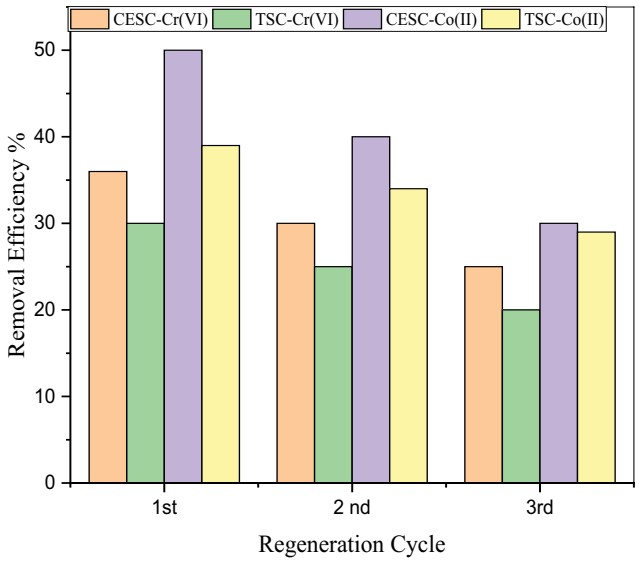

Fig. 15. Reusability studies of CESC and TSC.

streams. On the basis of the results of the multipoint BET calculations for CESC and TSC, their mean pore radii were 0.0106 and 0.696 nm, respectively, and their specific surface areas were 39.5 and 0.414 m^2/g, respectively. At the optimal experimental conditions (i.e., pH = 2 for Cr^{6+} and 4 for Co^{2+}, agitator speed = 100 rpm, contact time = 180 min, temperature = 30°C, and biosorbent dosage = 5 g/L), CESC and TSC exhibited maximum removal capacities of 200.64 and 187.78 mg/g for Cr^{6+} and 220.34 and 142.21 mg/g for Co^{2+}, respectively. The exothermic biosorption process was well explained using the Langmuir isotherm and pseudo-second-order kinetic model. The CESC and TSC biosorbents demonstrated good regeneration capacity up to three biosorption runs when regenerated using an HNO_3 solution. Thus, the CESC and TSC beads prepared in this study can be used as a solid-phase extractant for the removal of Cr^{6+} and Co^{2+} from aqueous solutions. Therefore, this research established a theoretical and experimental foundation for the use of TSC and CESC beads as a new adsorbent for the removal of Cr^{6+} and Co^{2+} ions from synthetic wastewater samples.

References

[1] D. Mohan, C.U. Pittman Jr., Activated carbons and low cost adsorbents for remediation of tri-and hexavalent chromium from water, J. Hazard Mater., 137 (2006) 762–811.

[2] V. Sarin, K.K. Pant, Removal of chromium from industrial waste by using eucalyptus bark, Bioresour. Technol., 97 (2006) 15–20.

[3] K. Zhu, C. Chen, H. Xu, Y. Gao, X. Tan, A. Alsaedi, T. Hayat, Cr(VI) reduction and immobilization by core-double-shell structured magnetic polydopamine@zeolitic idazolate frameworks-8 microspheres, ACS Sustainable Chem. Eng., 5 (2017) 6795–6802.

[4] K. Ravikumar, D. Kumar, A. Rajeshwari, G. Madhu, P. Mrudula, N. Chandrasekaran, A. Mukherjee, A comparative study with biologically and chemically synthesized nZVI: applications in Cr(VI) removal and ecotoxicity assessment using indigenous microorganisms from chromium-contaminated site, Environ. Sci. Pollut. Res., 23 (2016) 2613–2627.

[5] A. Zayed, C.M. Lytle, J.-H. Qian, N. Terry, Chromium accumulation, translocation and chemical speciation in vegetable crops, Planta, 206 (1998) 293–299.

[6] K. Ravikumar, S.V. Sudakaran, M. Pulimi, C. Natarajan, A. Mukherjee, Removal of hexavalent chromium using nano zero valent iron and bacterial consortium immobilized alginate beads in a continuous flow reactor, Environ. Technol. Innovation, 12 (2018) 104–114.

[7] K. Mulani, S. Daniels, K. Rajdeo, S. Tambe, N. Chavan, Adsorption of chromium(VI) from aqueous solutions by coffee polyphenol-formaldehyde/acetaldehyde resins, J. Polym., 2013 (2013) 798368, doi: 10.1155/2013/798368.

[8] H. Li, Z. Li, T. Liu, X. Xiao, Z. Peng, L. Deng, A novel technology for biosorption and recovery hexavalent chromium in wastewater by bio-functional magnetic beads, Bioresour. Technol., 99 (2008) 6271–6279.

[9] A.S. Yusuff, Adsorption of hexavalent chromium from aqueous solution by *Leucaena leucocephala* seed pod activated carbon: equilibrium, kinetic and thermodynamic studies, Arab J. Basic Appl. Sci., 26 (2019) 89–102.

[10] S. Hokkanen, A. Bhatnagar, A. Koistinen, T. Kangas, U. Lassi, M. Sillanpää, Comparison of adsorption equilibrium models and error functions for the study of sulfate removal by calcium hydroxyapatite microfibrillated cellulose composite, Environ. Technol., 39 (2018) 952–966.

[11] M. Qurie, M. Khamis, A. Manassra, I. Ayyad, S. Nir, L. Scrano, S.A. Bufo, R. Karaman, Removal of Cr(VI) from aqueous environments using micelle-clay adsorption, Sci. World J., 2013 (2013) 942703, doi: 10.1155/2013/942703.

[12] A. Kumar, H. Joshi, A.J.S. Kumar, P. Reviews, Remediation of arsenic by metal/metal oxide based nanocomposites/ nanohybrids: contamination scenario in groundwater, practical challenges, and future perspectives, Sep. Purif. Rev., 50 (2020) 1–32.

[13] M.M.E. Breky, E.H. Borai, A.T. Kassem, Synthesis of high-grade alumina from aluminium dross and its utilization for the sorption of radioactive cobalt, Desal. Water Treat., 170 (2019) 265–276.

[14] K. Rambabu, J. Al-Yammahi, G. Bharath, A. Thanigaivelan, N. Sivarajasekar, F. Banat, Nano-activated carbon derived from date palm coir waste for efficient sequestration of noxious 2,4-dichlorophenoxyacetic acid herbicide, Chemosphere, 282 (2021) 131103, doi: 10.1016/j.chemosphere.2021.131103.

[15] S. Nandhini, B. Samiha, S. Shwetha, G. Nirmala, T. Murugesan, K. Rambabu, A. Hatem, A. Faheem, S. Pau Loke, Continuous phenol removal using a liquid–solid circulating fluidized bed, Energies, 13 (2020) 3839, doi: 10.3390/en13153839.

[16] G. Bharath, J. Prakash, K. Rambabu, G.D. Venkatasubbu, A. Kumar, S. Lee, J. Theerthagiri, M.Y. Choi, F. Banat, Synthesis of TiO_2/RGO with plasmonic Ag nanoparticles for highly efficient photoelectrocatalytic reduction of CO_2 to methanol toward the removal of an organic pollutant from the atmosphere, J. Environ. Pollut., 281 (2021) 116990.

[17] H.R. Noormohamadi, M.R. Fat'hi, M. Ghaedi, G.R. Ghezelbash, Potentiality of white-rot fungi in biosorption of nickel and cadmium: modeling optimization and kinetics study, Chemosphere, 216 (2019) 124–130.

[18] K. Rambabu, A. Thanigaivelan, G. Bharath, N. Sivarajasekar, F. Banat, P.L. Show, Biosorption potential of *Phoenix dactylifera* coir wastes for toxic hexavalent chromium sequestration, Chemosphere, 268 (2021) 128809.

[19] S. Rangabhashiyam, E. Suganya, A.V. Lity, N. Selvaraju, Equilibrium and kinetics studies of hexavalent chromium biosorption on a novel green macroalgae *Enteromorpha* sp., Res. Chem. Intermed., 42 (2016) 1275–1294.

[20] K. Rambabu, G. Bharath, F. Banat, P.L. Show, Biosorption performance of date palm empty fruit bunch wastes for toxic hexavalent chromium removal, Environ. Res., 187 (2020) 109694.

[21] R. Rahman, H. Ibrahium, Y.-T. Hung, Liquid radioactive wastes treatment: a review, Water, 3 (2011) 551–565.

[22] P.A. Nishad, A. Bhaskarapillai, S. Velmurugan, S.V. Narasimhan, Cobalt(II) imprinted chitosan for selective removal of cobalt during nuclear reactor decontamination, Carbohydr. Polym., 87 (2012) 2690–2696.

[23] M.M.E. Breky, E.H. Borai, M.S.E. Sayed, M.M. Abo-Aly, Comparative sorption study of cesium, cobalt and europium

using induced gamma radiation polymeric nanocomposites, Desal. Water Treat., 116 (2018) 148–157.
[24] N. Yousefi, M. Jones, A. Bismarck, A. Mautner, Fungal chitin-glucan nanopapers with heavy metal adsorption properties for ultrafiltration of organic solvents and water, Carbohydr. Polym., 253 (2021) 117273.
[25] C. Gok, S. Aytas, Biosorption of uranium(VI) from aqueous solution using calcium alginate beads, J. Hazard. Mater., 168 (2009) 369–375.
[26] K.Y. Lee, D.J. Mooney, Alginate: properties and biomedical applications, Prog. Polym. Sci., 37 (2012) 106–126.
[27] J. Choi, Characterization of hydrogel made by pH-responsive polymer and alginate, Polymers, 41 (2017) 1046–1051.
[28] S. Chen, Y. Zou, Z. Yan, W. Shen, S. Shi, X. Zhang, H. Wang, Carboxymethylated-bacterial cellulose for copper and lead ion removal, J. Hazard. Mater., 161 (2009) 1355–1359.
[29] Q. Li, H. Su, T. Tan, Synthesis of ion-imprinted chitosan-TiO_2 adsorbent and its multi-functional performances, Biochem. Eng. J., 38 (2008) 212–218.
[30] D. Kanakaraju, S. Ravichandar, Y.C. Lim, Combined effects of adsorption and photocatalysis by hybrid TiO_2/ZnO-calcium alginate beads for the removal of copper, J. Environ. Sci., 55 (2017) 214–223.
[31] D. Chen, A.K. Ray, Removal of toxic metal ions from wastewater by semiconductor photocatalysis, Chem. Eng. Sci., 56 (2001) 1561–1570.
[32] X. Wang, S. Pehkonen, A.K. Ray, Removal of aqueous Cr(VI) by a combination of photocatalytic reduction and coprecipitation, Ind. Eng. Chem. Res., 43 (2004) 1665–1672.
[33] M. López-Muñoz, J. Aguado, A. Arencibia, R. Pascual, Mercury removal from aqueous solutions of $HgCl_2$ by heterogeneous photocatalysis with TiO_2, Appl. Catal., B, 104 (2011) 220–228.
[34] S. Satyro, R. Marotta, L. Clarizia, I. Di Somma, G. Vitiello, M. Dezotti, G. Pinto, R.F. Dantas, R. Andreozzi, Removal of EDDS and copper from waters by TiO_2 photocatalysis under simulated UV–solar conditions, Chem. Eng. J., 251 (2014) 257–268.
[35] C.D. Murphy, Drug metabolism in microorganisms, Biotechnol. Lett., 37 (2015) 19–28.
[36] V. Tigini, V. Prigione, I. Donelli, A. Anastasi, G. Freddi, P. Giansanti, A. Mangiavillano, G.C. Varese, *Cunninghamella elegans* biomass optimisation for textile wastewater biosorption treatment: an analytical and ecotoxicological approach, Appl. Microbiol. Biotechnol., 90 (2011) 343–352.
[37] A. Abdel-Razek, T. Abdel-Ghany, S. Mahmoud, H. El-Sheikh, M. Mahmoud, The use of free and immobilized *Cunninghamella elegans* for removing cobalt ions from aqueous waste solutions, World J. Microbiol. Biotechnol., 25 (2009) 2137.
[38] P.T. Williams, A. Reed, Development of activated carbon pore structure via physical and chemical activation of biomass fibre waste, Biomass Bioenergy, 30 (2006) 144–152.
[39] A.-F. Ngomsik, A. Bee, J.-M. Siaugue, D. Talbot, V. Cabuil, G. Cote, Co(II) removal by magnetic alginate beads containing Cyanex 272®, J. Hazard. Mater., 166 (2009) 1043–1049.
[40] Y. Sharma, V. Srivastava, A. Mukherjee, Synthesis and application of nano-Al_2O_3 powder for the reclamation of hexavalent chromium from aqueous solutions, J. Chem. Eng. Data, 55 (2010) 2390–2398.
[41] Y.S. Al-Degs, M.I. El-Barghouthi, A.H. El-Sheikh, G.M. Walker, Effect of solution pH, ionic strength, and temperature on adsorption behavior of reactive dyes on activated carbon, Dyes Pigm., 77 (2008) 16–23.
[42] I. Langmuir, The adsorption of gases on plane surfaces of glass, mica and platinum, J. Am. Chem. Soc., 40 (1918) 1361–1403.
[43] H. Freundlich, Over the adsorption in solution, J. Phys. Chem., 57 (1906) 1100–1107.
[44] S. Bo, W. Ren, C. Lei, Y. Xie, Y. Cai, S. Wang, J. Gao, Q. Ni, J. Yao, Flexible and porous cellulose aerogels/zeolitic imidazolate framework (ZIF-8) hybrids for adsorption removal of Cr(IV) from water, J. Solid State Chem., 262 (2018) 135–141.
[45] K. Rambabu, B. Fawzi, G. Nirmala, S. Velu, P. Monash, G. Arthanareeswaran, Activated carbon from date seeds for chromium removal in aqueous solution, Desal. Water Treat., 156 (2019) 267–277.
[46] S.K. Lagergren, About the theory of so-called adsorption of soluble substances, Sven. Vetenskapsakad. Handingarl, 24 (1898) 1–39.
[47] Y.-S. Ho, G. McKay, Pseudo-second-order model for sorption processes, Process Biochem., 34 (1999) 451–465.
[48] W. Shen, Q.-D. An, Z.-Y. Xiao, S.-R. Zhai, J.-A. Hao, Y. Tong, Alginate modified graphitic carbon nitride composite hydrogels for efficient removal of Pb(II), Ni(II) and Cu(II) from water, Int. J. Biol. Macromol., 148 (2020) 1298–1306.
[49] G. Asgari, A.R. Rahmani, J. Faradmal, M.A. Seid, Kinetic and isotherm of hexavalent chromium adsorption onto nano hydroxyapatite, J. Health Sci. Res., 12 (2012) 45–53.
[50] Y.-y. Wang, W.-b. Yao, Q.-w. Wang, Z.-h. Yang, L.-f. Liang, L.-y. Chai, Synthesis of phosphate-embedded calcium alginate beads for Pb(II) and Cd(II) sorption and immobilization in aqueous solutions, Trans. Nonferrous Met. Soc., 26 (2016) 2230–2237.
[51] W.M. Algothmi, N.M. Bandaru, Y. Yu, J.G. Shapter, A.V. Ellis, Alginate–graphene oxide hybrid gel beads: an efficient copper adsorbent material, J. Colloid Interface Sci., 397 (2013) 32–38.
[52] A. Ahmad, A. Bhat, A. Buang, Biosorption of transition metals by freely suspended and Ca-alginate immobilised with *Chlorella vulgaris*: kinetic and equilibrium modeling, J. Cleaner Prod., 171 (2018) 1361–1375.
[53] L. Xu, J. Wang, The application of graphene-based materials for the removal of heavy metals and radionuclides from water and wastewater, Crit. Rev. Env. Sci. Technol., 47 (2017) 1042–1105.
[54] A. Omer, R. Khalifa, Z. Hu, H. Zhang, C. Liu, X.-k. Ouyang, Fabrication of tetraethylenepentamine functionalized alginate beads for adsorptive removal of Cr(VI) from aqueous solutions, Int. J. Biol. Macromol., 125 (2019) 1221–1231.
[55] Y. Zhu, J. Hu, J. Wang, Removal of Co^{2+} from radioactive wastewater by polyvinyl alcohol (PVA)/chitosan magnetic composite, Prog. Nucl. Energy, 71 (2014) 172–178.
[56] S. Bhattarai, J.S. Kim, Y.-S. Yun, Y.-S. Lee, Thiourea-immobilized polymer beads for sorption of Cr(VI) ions in acidic aqueous media, Macromol. Res., 27 (2019) 515–521.
[57] S. Zhuang, Y. Yin, J. Wang, Simultaneous detection and removal of cobalt ions from aqueous solution by modified chitosan beads, Int. J. Environ. Sci. Technol., 15 (2018) 385–394.
[58] T. Altun, Chitosan-coated sour cherry kernel shell beads: an adsorbent for removal of Cr(VI) from acidic solutions, J. Anal. Sci. Technol., 10 (2019) 14.
[59] H. Chen, D. Shao, J. Li, X. Wang, The uptake of radionuclides from aqueous solution by poly (amidoxime) modified reduced graphene oxide, Chem. Eng. J., 254 (2014) 623–634.
[60] E.-h. Ablouh, Z. Hanani, N. Eladlani, M. Rhazi, M. Taourirte, Chitosan microspheres/sodium alginate hybrid beads: an efficient green adsorbent for heavy metals removal from aqueous solutions, Sustainable Environ. Res., 29 (2019) 1–11.
[61] W. Jung, B.-H. Jeon, D.-W. Cho, H.-S. Roh, Y. Cho, S.-J. Kim, D.S. Lee, Sorptive removal of heavy metals with nano-sized carbon immobilized alginate beads, J. Ind. Eng. Chem., 26 (2015) 364–369.
[62] G.Z. Kyzas, Commercial coffee wastes as materials for adsorption of heavy metals from aqueous solutions, J. Mater., 5 (2012) 1826–1840.